Proceedings, Bicycle and Motorcycle Dynamics 2019
Symposium on the Dynamics and Control of Single Track Vehicles,
9–11 September 2019, University of Padova, Italy

# Rider model for the estimation of tyre forces in off-road motorcycles

**F. Vasquez*, R. Lot#, E. Rustighi†, R. Pegoraro‡**

* Mechanical Engineering Department
University of Southampton
University Rd, SO171BJ Southampton, UK
e-mail: F.A.Vasquez-Stuardo@soton.ac.uk

# Mechanical Engineering Department
University of Southampton
University Rd, SO171BJ Southampton, UK
e-mail: Roberto.Lot@soton.ac.uk

† Institute of Sound and Vibration Research
University of Southampton
University Rd, SO171BJ Southampton, UK
e-mail: er@isvr.soton.ac.uk

‡ Off-road Racing Division
WP Suspension
A-5230, Mattighofen, Austria
e-mail: Roberto.Pegoraro@wp-racing.com

## ABSTRACT

The estimation of tyre forces in off-road motorcycle is required to measure objectively its performance. It requires the interaction between motorcycle and the rider in standing position. The existing rider model for off-road motorcycles is computationally expensive and it has not been validated. In this article we present a model for a standing rider based on observed kinematics and tested it with experimental data collected on a motocross track. Results shows that the rider-motorcycle forces are calculated in a negligible time and furthermore are more realistic than with the previous model. When used in the estimator, the forces were mostly similar, and in discrepancies, the estimations with the simpler model were more realistic.

**Keywords:** Motorcycle Dynamics, Rider Model, Tyre Force Estimation, Off-Road.

## 1 INTRODUCTION

Off-road motorcycle can transit over roads with significant irregularities and elevation changes. The impulses from the road are absorbed by the suspension system and by the rider driving in standing position. The rider's mass contribution to motorcycle-rider system is non-negligible [1], therefore, a rider model is required.

Existing rider models usually focus on control strategies [2] [3], (see [1] for a review). They consider the rider in seated position, since were developed for on road conditions. Differently, in off-road, since transit is in standing position, the rider's arms and legs provide significant vibration isolation and hence they should be included as model components [4]. Multibody rider models for off-road bicycles were developed by Wilczynski[5] and Wang [4] to estimate frame loads.

Recognizing the similar driving techniques used by drivers in off-road bicycles and motorcycles, the authors [6] proposed a simplified version of the bicycle models to estimate off-road motorcycle tyre forces. This estimation process consists on two steps. First, the differential equations of motion of the rider are integrated to calculate the rider forces, and second, the algebraic inverse equations of motion of the motorcycle are solved to calculate the tyre forces. With a processor of to 2.5 GHz and 8 Gb RAM, the rider model takes about 5 times the real time of the data sampled at 1.6 kHz, while the second steps takes only 0.5 times. Furthermore, it has not being validated experimentally, nor on the parameters used, since we have taken the ones from bicycles,

which were measured for smaller road amplitudes [5], consequently there is no certainty on the estimation,

Given that the rider is an important component of the overall motorcycle dynamics and that the current available model for off-road, is computationally expensive and moreover there is no certainty on its validity, the rider model for off-road motorcycle is an open question.

In this article, we present a simple rider model which describes the dynamics with algebraic expressions by assuming the rider kinematics instead of obtaining them from integration of the equations of motion. This removes the need of integration of the previous model, making the computation time practically negligible, while still being representative of the rider-motorcycle interaction. In section 2, we briefly present the tyre force estimator in which the rider forces are needed; in section 3, we describe the previous rider model and present the simpler one. In section 4, we use experimental data collected on a motocross track to compare the rider forces and the estimated tyre forces yield with both. Finally, we discuss limitations and summarize main conclusions.

## 2 INVERSE DYNAMICS METHOD FOR TYRE FORCE ESTIMATION

In this section a tyre force estimator, developed for off-road conditions is described. We consider the problem of calculating the tyre forces using a multibody description of the motorcycle, assuming that kinematic variables are known from experimental measurements. To process the experimental data as efficiently as possible, we derive and manipulate a set of symbolic equations using MBSymba, [7, 8, 9] which is an add-on for Maple [10]. To compensate for measurement errors, we derive an overdetermined system and to further improve the results, we add a set of constraints equations. Finally we solve for the tyre forces using a non-negative least squares method.

### 2.1 Motorcycle equations of motion

The equations of motion of the motorcycle are derived under the following four assumptions. First, we consider in plane motion only, since our interest is mainly on manoeuvres such as braking and accelerating, Figure 1. Second, by neglecting structural vibrations, we can represent the motorcycle by four interconnected bodies with five degrees of freedom, which are described by as many coordinates,

$$\mathbf{q} = [x_s, z_s, \mu, z_f, \alpha_r]^T, \tag{1}$$

where, $x_s$ and $z_s$ are horizontal and vertical displacement of the chassis centre of mass, $\mu$ is chassis rotation, $z_f$ is the front suspension compression, and $\alpha_r$ is the rear suspension compression defined as the relative rotation between swingarm and chassis. Third, since the manoeuvres of interest are generally transited in standing position, we consider that the rider interacts with the handlebar and foot pegs only. Fourth, the contact point with the ground is considered to be directly under the wheel centre as seen in nominal condition. This implies that the contact point does not move forward or backwards due to road irregularities, and therefore, normal and tangential components are always aligned with $z_3$ and $x_3$ axis, respectively. This simplification is based on the observation that only when transiting large obstacles, such as *whoops* in Figure 3, the contact points move significantly from the bottom of the tyres. In this way, the estimation of the contact point position, which is not a trivial task, is avoided and there are only four tyre force components to be determined.

We derive five equations of motions, one for each degree of freedom, and collect them as

$$\mathbf{M}\ddot{\mathbf{q}} + \mathbf{m_v} = \mathbf{A_w}g + \mathbf{A_s}\mathbf{f_s} + \mathbf{A_r}\mathbf{f_r} + \mathbf{A_t}\mathbf{f_t}, \tag{2}$$

where, $\mathbf{M}$ is the mass matrix, $\ddot{\mathbf{q}}$ is the acceleration vector, $g$ is gravity acceleration, $\mathbf{f_s},\ \mathbf{f_r},\ \mathbf{f_t}$ are suspension, rider and tyre force vectors respectively and the matrices $\mathbf{A_w},\ \mathbf{A_s},\ \mathbf{A_r},\ \mathbf{A_t}$ project

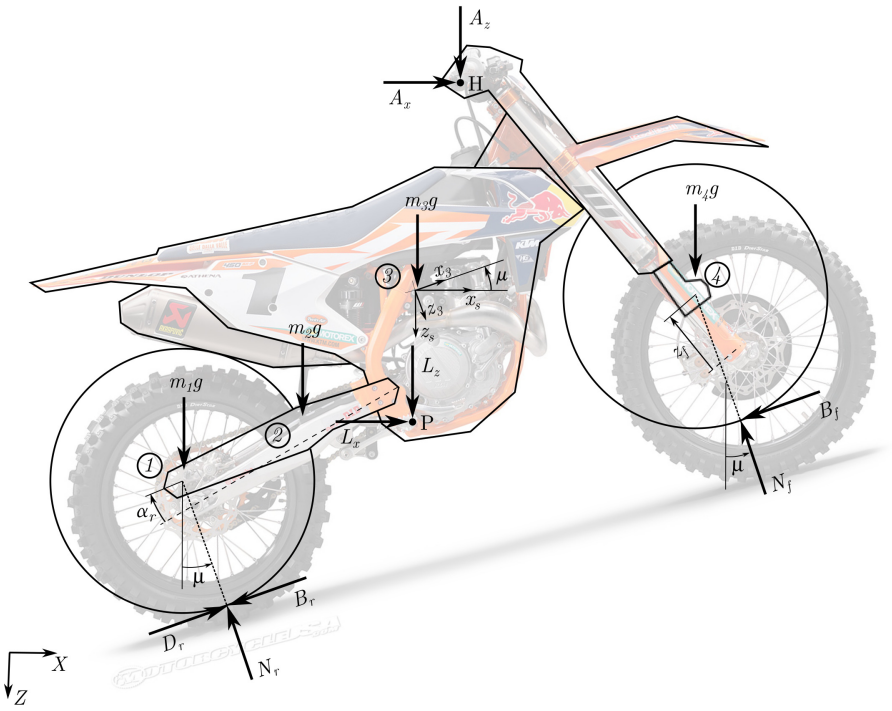


**Figure 1**. Motorcycle model. $x_s$, $z_s$ and $\mu$ are horizontal, vertical and angular position of chassis centre of mass; $z_f$ is fork compression, and $\alpha_r$ is swing arm angular compression; $A_x$, $A_z$, $L_x$, $L_z$ are rider's arm and leg forces acting over the handlebar (H) and foot-peg (P); $N_r$ and $N_f$ are normal forces over the tyres assumed to be along the $z_3$, which is tilted $\mu$ from absolute vertical; $B_r$, $B_f$ are rear and front braking force and $D_r$ is rear driving force which are assumed to be along chassis x-axis.

these forces along each of the five coordinates. $\mathbf{m_v}$ is the pseudo-mass vector which contains relative acceleration terms, and also the product of wheels rotational inertia by their angular accelerations. We did not model wheel rotations as coordinates in $\mathbf{q}$ since we can measure them directly to represent the rotational inertia effect and therefore, we did not need to derive equations of motion for them. See Appendix A, for explicit description of matrices and vectors.

In Equation (2), masses , rotational inertias, and geometry in $\mathbf{M}, \mathbf{m_v}$ and projection matrices can be measured with no major complication. Accelerations in $\ddot{\mathbf{q}}$, velocities and angular acceleration in $\mathbf{m_v}$, and positions can be measured with accelerometers, potentiometers and tachometers or derived from them; suspension forces $\mathbf{f_s}$ can be estimated from characterisation of the spring and damper; and the rider forces $\mathbf{f_r}$ can be estimated as described on Section 3.

Acknowledging the presence of measurement errors, we derive an overdetermined system to reduce them. In particular, Equation (2) consist of five equations to determine four unknown tyre force components.

### 2.2 Constraints of the optimisation

The overdetermined system can not compensate the measurement errors completely and non-physical solutions can be obtained regardless. To reduce these non-physical solutions, we add equality and inequality constraints to the optimisation.

On one hand, we add inequality constraints to consider that normal forces and front tangential force (braking) can physically exist in one direction only. By defining the rear tangential force as two non-negative forces as well, we add the constraints,

$$\mathbf{f_t} = [N_f \; N_r \; B_f \; B_r \; D_r]^T \geq \mathbf{0}, \tag{3}$$

where, $N_f$ and $N_r$ are normal forces on front and rear tyres; $B_f$ and $B_r$ are braking forces on front and rear tyre; and $D_r$ is the driving force on the rear tyre. In this way, there are five variables to be determined, nonetheless, the problem still has four unknowns, since by definition only $D_r$ or $B_r$ exist at anytime.

On the other hand, we add equality constrains to impose a solution when some terms are known under certain driving conditions. These are: $N_f = B_f = 0$ when front wheel is detached; $N_r = B_r = D_r = 0$ when rear wheel is detached; $B_f = B_r = 0$, when motorcycle is driving (accelerating); and $D_r = 0$ when braking. In order to impose these constraints only under the corresponding conditions, we multiply each constraint equation by an activation weight, $W_{ii}$, that is 1 when the condition is satisfied, and 0, otherwise. In this way, we express the constraints as

$$\mathbf{W}\mathbf{f_t} = \mathbf{0}, \tag{4}$$

where $\mathbf{W} = \text{diag}(W_{ii})$.

### 2.3 Solution of the inverse dynamic problem

The five Equation (2) can not be satisfied simultaneously by any vector $\mathbf{f_t}$ due random errors on the measurements. Then, an alternative approach, is to find $\mathbf{f_t}$ such that it minimizes $\mathbf{A}\mathbf{f_t} - \mathbf{b_1}$, where $\mathbf{b_1} = \mathbf{M}\ddot{\mathbf{q}} + \mathbf{m_v} - \mathbf{A_w}g - \mathbf{A_s}\mathbf{f_s} - \mathbf{A_r}\mathbf{f_r}$ are the known terms. Considering the constraints, the problem is the optimisation

$$\begin{aligned} &\text{find } \mathbf{f_t} \text{ that :} \\ &\quad \min_{\mathbf{f_t}} \; \|\mathbf{B}(\mathbf{A}\mathbf{f_t} - \mathbf{b})\| \,, \\ &\text{subject to:} \quad \mathbf{f_t} \geq \mathbf{0}, \end{aligned} \tag{5}$$

where,

$$\mathbf{B} = \begin{bmatrix} \mathbf{B_d} & \mathbf{0} \\ \mathbf{0} & \mathbf{B_c} \end{bmatrix}, \quad \mathbf{A} = \begin{bmatrix} \mathbf{A_t} \\ \mathbf{W} \end{bmatrix}, \quad \mathbf{b} = \begin{bmatrix} \mathbf{b_1} \\ \mathbf{0} \end{bmatrix}. \tag{6}$$

In this formulation, three considerations are taken. First, $\mathbf{f_t}$ is solved in the least squares sense. Second, the equality constraint $\mathbf{W f_t} = \mathbf{0}$ are appended to the dynamic equations with a heavy weight $\mathbf{B_c}$, since it allows the constraints not to be met exactly, which serves to compensate errors in the transitions from active to inactive constraints. Third, difference in uncertainties between dynamic equations can be taken into account by the weights in $\mathbf{B_d}$.

Equation (5) is a non-negative least squares problem, which is solved numerically by the Lawson-Hanson algorithm for non-negative problems, presented in [11], and implemented in MATLAB [12] as `lsqnonneg`.

## 3 RIDER FORCES

In this section, the rider model presented by the authors in [6] is briefly described, which is followed by the presentation of a simpler rider model. The former rider is referred as Rider A, while the latter as Rider B, to simplify notation.

Rider A consists on one body connected to the motorcycle by arms and legs modelled with springs and dampers, Figure 2a. Two main assumptions were made. First, forces of arms and legs can be represented by passive elements, which are assumed to act between shoulder-handlebar and hip-foot peg directions respectively. Second, since it is observed that while riding the absolute rotation is small compared to vertical and horizontal translations, a hip torque is added to keep the angle constant. This torque is calculated from Euler's equation on the torso's $y-$axis to cancel-out the torque produced by arm and leg forces. The calculation of the forces is done in two steps. First, the kinematics of the rider is determined by integrating the equation of motion

$$\dot{\mathbf{x}}_\mathbf{A} = [\ddot{x}_A \ \ddot{z}_A \ \dot{x}_A \ \dot{z}_A]^T = \mathbf{g}(\mathbf{x_A}, \mathbf{u}) \tag{7}$$

which are based on the chassis motion $\mathbf{u}$, and subsequently, the forces, are retrieved from the spring and damper models of arms and legs,

$$\mathbf{f_{r,A}} = [L_x \ L_z \ A_x \ A_z]_A^T = \mathbf{h}(\dot{\mathbf{x}}_\mathbf{A}, \mathbf{x_A}, \mathbf{u}). \tag{8}$$

Rider B, Figure 2b, is developed taking into consideration two situations. First, observation of the rider driving in irregular roads shows that the centre of gravity, which is approximately in the hip, is almost on a constant vertical position (Figure 3), therefore velocity and acceleration are small ($\dot{z}_B \approx 0$ and $\ddot{z}_B \approx 0$), which implies that arm and leg vertical forces are close to equilibrium with rider's weight, and consequently, are close to constant. Second, in braking and acceleration, his/her centre of mass barely moves horizontally with respect to the chassis, which implies that their horizontal accelerations should be similar ($\ddot{x}_B \approx \ddot{x}_s$). Consequently, the total vertical and horizontal forces over the rider can be approximated as the weight and the horizontal inertial force, respectively. In order to further simplify the representation, we assume that the vertical force is completely exerted through the legs, and the horizontal force, by the arms, resulting in

$$\mathbf{f_{r,B}} = [L_x \ L_z \ A_x \ A_z]_B^T = [0 \ m_r g \ -m_r \ddot{x}_s \ 0]^T. \tag{9}$$

Additionally, we consider that all components are zero if contact is lost in front and rear wheels simultaneously.

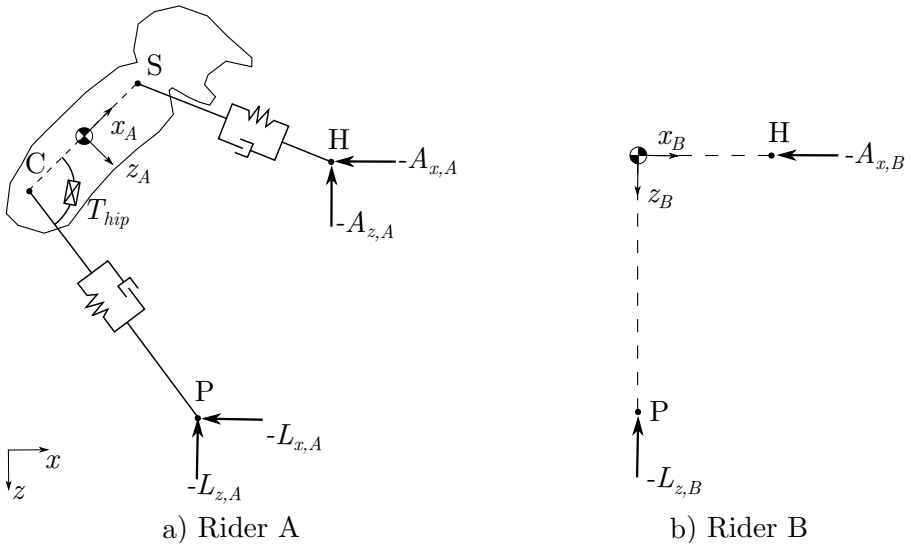


**Figure 2**. Rider models. Rider A consist on one body connected to the motorcycle by arm and legs, assumed to act passively, and a torque on the hip, $T_{hip}$, that keeps the torso angle constant. The motion of handlebar (H) and foot-peg's (P) excite the rider, and from the spring and dampers models of arms and legs, the forces are retrieved. Differently, Rider B consist on two forces explicitly defined on terms of chassis motion ($\ddot{x}_s$).

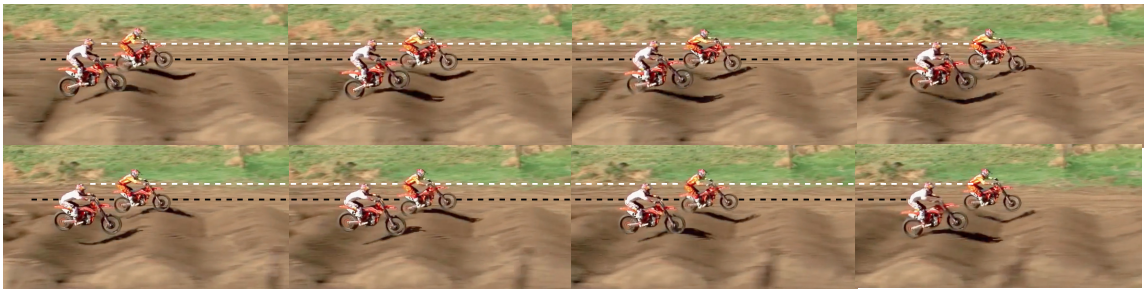

**Figure 3**. Two motorcycles riding through *whoops* section. It shows that although the riders moves broadly, the vertical position of their hips shown in white and black dashed lines, remains roughly at the same height [13].

The underlying difference between both models, is where the assumptions are made. On Rider A, they are made on the equations of motion that calculate the kinematics, while on Rider B, they are made directly on the kinematics. The consequence of this is that Rider A can potentially represent accurately the kinematics, but it can also diverge significantly from reality if any significant phenomena is being omitted from the equations. Conversely, on Rider B by representing only its broad motion, it may not be accurate, but at least is similar to the real motion. Taking into account that the forces depend on the motion, Rider A might provide a very close as well as very far estimation of rider-motorcycle forces, while Rider B, although not exact, it is relatively similar to the real interaction.

## 4 PERFORMANCE WITH EXPERIMENTAL DATA

The performance of both rider models are compared using data collected with a motocross motorcycle on three driving conditions. First, we compare arm and leg forces of both rider models. Then, we use these forces as inputs for the estimator described in Section 2, to compare the estimated tyre forces.

Data is collected using a 2017 motocross motorcycle driven by a professional driver on a motocross track. The following thirteen measurement are collected to compute ten out of seventeen kinematic variables required by the estimator. An inertial unit under the seat measures chassis vertical acceleration, pitch angle, and forward velocity (GPS); accelerometers located on steering head and tail aligned with $z_3$ axis are used to compute chassis pitch acceleration as the ratio between the difference measured by them and their distance; a potentiometer aligned with the fork and an accelerometer at each end measures fork compression and compression acceleration, respectively; similarly, the rear spring-damper unit compression and acceleration are measured with a potentiometer and accelerometers at each end, which are then translated into rear suspension compression angle using the relationship between spring versus angle displacements, see [14] for details on the procedure; tachometers are used to measure wheel angular velocities. The remaining seven variables are obtained by numerical integration or differentiations of the measured variables. Integrations are performed by trapezoidal method with previous removal of signal mean to avoid drift, and differentiations are performed by a finite impulse response filter with delay compensation. Lastly, the signals are band-pass filtered with a custom made filter using Fourier and Inverse Fourier Transforms. Low-cut frequency on positions and forward velocity is the lowest positive frequency, to maintain the signal mean which physically exists on them, while on the rest, is set to zero, since if a mean exists, is due to noise. As high cut-off frequency, $20$ Hz is used to remove engine structural vibrations.

Three diverse driving conditions are selected to analize the performance of the rider models. First situation consist on two consecutive jumps of $\approx 0.8$ s flying time; second situation consist on ten bumps usually referred as *whoops*; and third situation is a cornering manoeuvre which includes braking and exit acceleration phases.

The forces of the riders on each situation are shown in Figure 4. It can be seen that Rider A forces are significantly larger and more oscillatory than Rider B forces. For example, on landings of Jumps ($t = 1$ and $t = 2.8$ s), $L_z$ and $A_x$ are about 4 and 6 times larger; and on cornering, $A_x$ oscillates seven times more. These forces are unlikely to be representative of reality, in first instance because forces of more than 3000N, (1500 N on each limb) can hardly be resisted by hands or feet, and second, if they would, it would imply large motions of the rider, which is not observed in reality. This unrealistic motion of Rider A, which explains the unrealistic forces implies that a significant phenomenon has been omitted from the equations, and which presumably is the active control exerted by a real driver. Increasing the damping, not shown here, reduces the oscillations but increases the magnitude of forces. Conversely, Rider B yields reasonable forces,

as expected.

The result of using both riders into the tyre forces estimator, are shown in Figure 5. In broad terms, it can be seen that the estimations are similar and in most of the disagreements, forces with Rider A are larger. In Jumps, normal forces, and the driving force before them, are similarly estimated with both riders, though with Rider A, $N_f$ and $D_r$ are about two times larger. In *whoops*, peaks in normal forces and the sequence braking-driving-braking are detected with both riders. Disagreements are seen in $B_r$ and $D_r$ which are higher with Rider A, and in $N_f$, where there are extra peaks estimated with Rider A. In cornering, braking and driving forces, as well as load transfers due to these forces, are in good agreement with both rider models. The major discrepancies are seen on $D_r$ and $B_r$ which are more oscillatory with Rider A. Considering that the rider forces are linear in the equations of motion of the estimator, it is expected to obtain larger and more oscillatory forces with Rider A. However, since the equations of motion are solved in the least squares sense, these larger forces are compensated to fit the remaining data of the equations.

It must be noted that in Rider B the most basic kinematic was assumed, namely, no vertical motion, and the horizontal as the motorcycle. However, in reality, the rider translates vertically on jumps, which implies that a larger force than his/her weight is required to pushing him/her up on the launch and also on the landing, consequently higher tyre forces are also expected on this instants. This could be taken into account by considering the vertical position of the chassis with a low-pass filter to take into account the vibration isolation provided by arms and legs.

In summary, it was found that the simpler rider provides a more realistic description of the rider-motorcycle interaction, which lead to a slightly more realistic estimation of the tyre forces. Furthermore, the calculation time with the simpler rider was reduced to almost negligible, permitting the estimation of tyre forces on real-time which opens the way to implement it on-board.

## 5 CONCLUSIONS

In this article we have presented a simple rider model to estimate tyre forces in off-road motorcycles. It is based on assumptions on the rider kinematics, which removes the integration step used on the previous model to determine the kinematics. This reduces the calculation time and also improves the representation of the rider-motorcycle interaction. Tested with experimental data, the simpler model showed forces more representative of reality that the previous model. When used as input for an estimator of contact forces, the estimations were similar with both models, and in discrepancies, the estimations with the simpler model were more realistic.

## ACKNOWLEDGEMENTS

F. Vasquez is grateful to the Chilean agency for science and technology, CONICYT, for founding received to pursue a doctoral program.

## REFERENCES

[1] Popov, A., Rowell, S., and Meijaard, J. (2010) A review on motorcycle and rider modelling for steering control. Vehicle System Dynamics: International Journal of Vehicle Mechanics and Mobility,.

[2] Massaro, M. (2011) A nonlinear virtual rider for motorcycles. Vehicle System Dynamics: International Journal of Vehicle Mechanics and Mobility, **49**(9), 1477–1496.

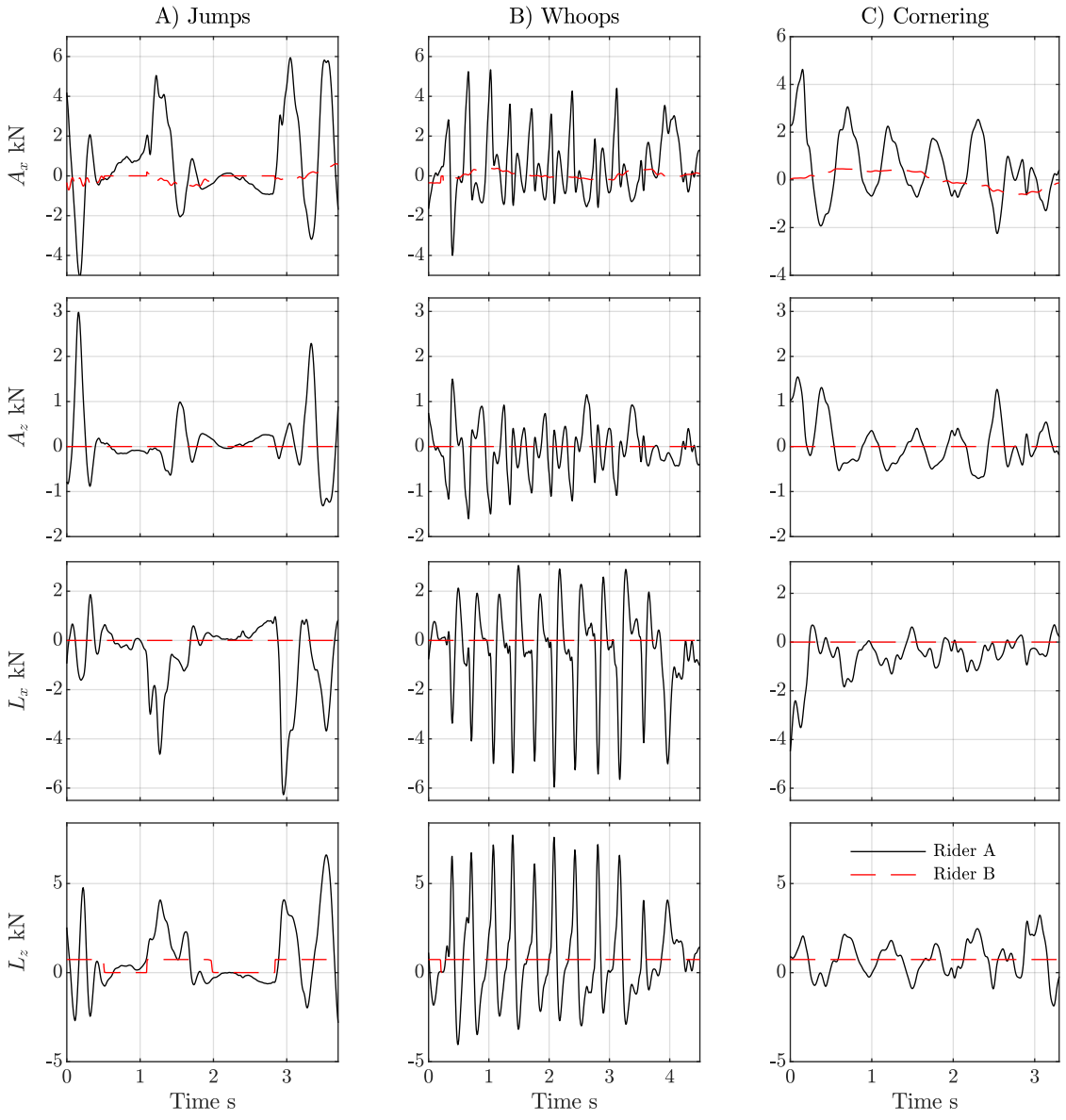


**Figure 4**. Rider forces estimated two rider models with data collected at a motocross track. Rider A dynamics are modelled with passive elements and requires simultaneous integration of two equations of motion, Rider B dynamics are proportional to motorcycle measurements.

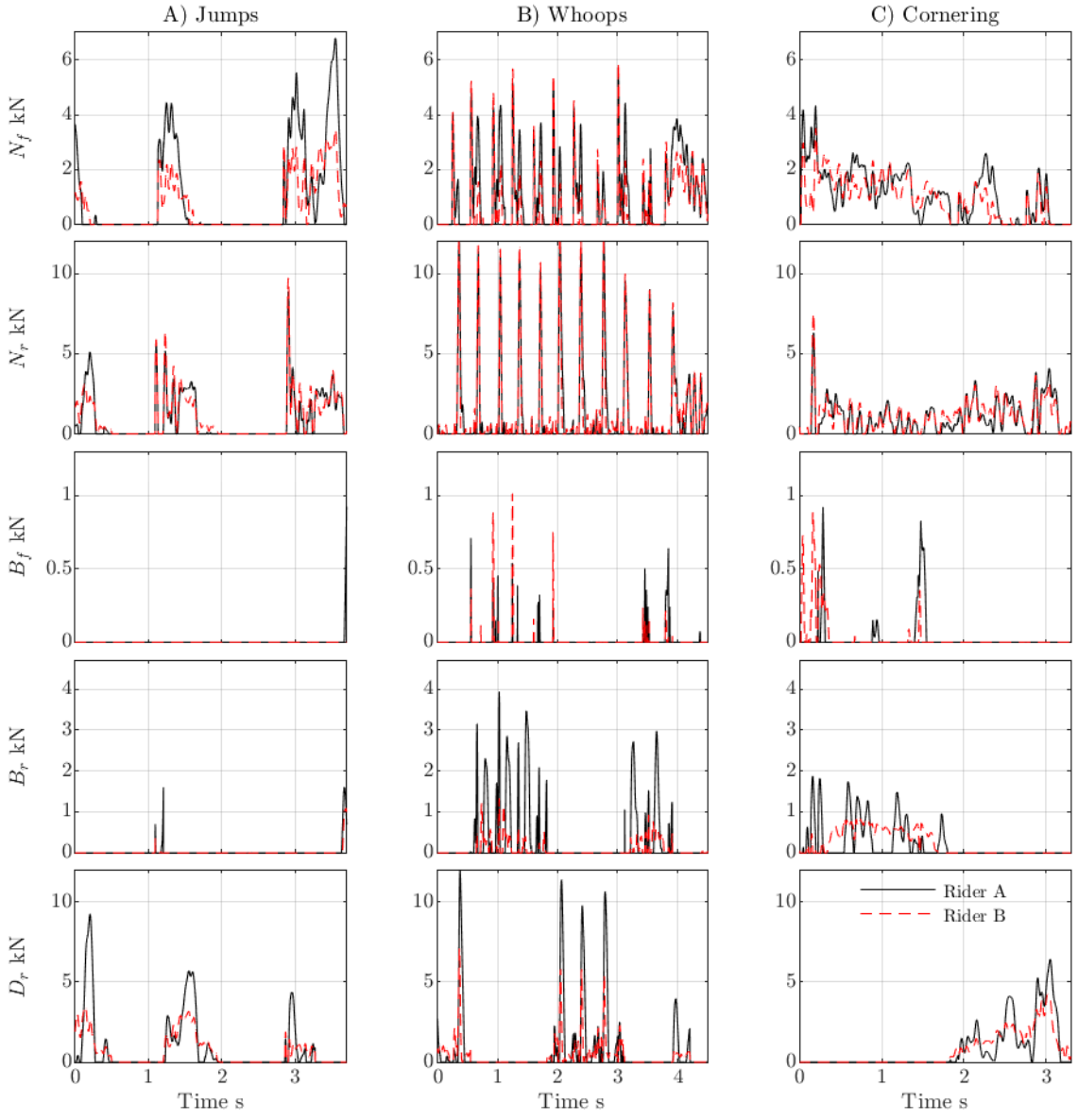


**Figure 5**. Contact forces estimated with both rider models. In general similar, but Rider A shows larger and more oscillatory forces than Rider B.

**Table 1**. Rider parameters. Rider A parameters are extracted from [5].

.

| | Rider A | Rider B | |
|---|---|---|---|
| Mass | 75 | 75 | kg |
| Arm stiffness | 23100 | - | N/m |
| Leg stiffness | 74000 | - | N/m |
| Arm damping | 515 | - | Ns/m |
| Leg damping | 1350 | - | Ns/m |


[3] Lot, R., Massaro, M., and Sartori, R. (2008) Advanced motorcycle virtual rider. Vehicle System Dynamics: International Journal of Vehicle Mechanics and Mobility, **46**, 215–224.

[4] Wang, E. and Hull, M. (1997) A dynamic system model of an off-road cyclist. Journal of Biomechanical Engineering, **119**, 248–253.

[5] Wilczynski, H. (1994) A dynamic system model for estimating surface-induced frame loads during off-road cycling. Journal of Mechanical Design, **116**, 816 – 822.

[6] Vasquez, F., Lot, R., and Rustighi, E. (2019) Off-Road motorcycle tyre force estimation. In Proceedings of the 13th International Conference on Recent Advances in Structural Dynamics.

[7] Lot, R. and da Lio, M. (2004) A Symbolic Approach for Automatic Generation of the Equations of motion of Multibody Systems. Multibody System Dynamics, **12**(2), 147–172.

[8] www.multibody.net. (May, 2019).

[9] Lot, R. and Massaro, M. (2017) A Symbolic Approach to the Multibody Modeling of Road Vehicles. International Journal of Applied Mechanics, **09**(05).

[10] www.maplesoft.net. (May, 2019).

[11] Lawson, C. and Hanson, J. (1974) Solving Least-Sqaures Problems, Prentice Hall, .

[12] www.mathworks.com. (May, 2019).

[13] https://youtu.be/NTqFmdJxWmI. (May, 2019).

[14] Cossalter, V. (2006) Motorcycle Dynamics, Lulu, .

**Table 2**. List of symbols. Sub-index $i$ refers to $f$ or $r$ for front or rear; sub-index $j$, refers to $x$ and $z$ directions; and sub-index $k \in [1, 2, 3, 4]$, refers to rear wheel, swing arm, chassis, and front wheel, respectively

| | |
|---|---|
| $\mathbf{A}$ | Generalized projection matrix |
| $\mathbf{A_r}$ | Rider force projection matrix |
| $\mathbf{A_s}$ | Suspension force projection matrix |
| $\mathbf{A_t}$ | Tyre force projection matrix |
| $\mathbf{A_w}$ | Weights projection matrix |
| $\mathbf{B}$ | Generalized weight matrix |
| $\mathbf{B_c}$ | Relative constraint eq. weight matrix |
| $\mathbf{B_d}$ | Relative dynamic eq. weight matrix |
| $\mathbf{M}$ | Mass matrix |
| $\mathbf{W}$ | Constraint activation weights matrix |
| $\mathbf{b}$ | Generalized known forces vector |
| $\mathbf{b_1}$ | Known forces vector |
| $\mathbf{f_r}$ | Rider forces vector |
| $\mathbf{f_s}$ | Suspension forces vector |
| $\mathbf{f_t}$ | Tyre contact forces vector |
| $\mathbf{m_v}$ | pseudo-mass vector |
| $\mathbf{q}$ | Motorcycle coordinates vector |
| $A_j$ | Arm forces along direction j |
| $B_i$ | Braking force on tyre i |
| $D_i$ | Driving force on tyre i |
| $L_j$ | Leg forces along direction j |
| $N_i$ | Normal force on tyre i |
| $X$ | Ground forward axis |
| $Z$ | Ground downward axis |
| $b$ | X distance between body 1 and 3 |
| $h$ | Height of chassis CoM |
| $I_k$ | Rotational inertia of body $k$ |
| $l_r$ | Distance from body 1 to swing arm main pin |
| $l_s$ | Distance from swing arm main pin to its CoM |
| $m$ | Total vehicle mass |
| $m_k$ | Mass of body $k$ |
| $m_r$ | Rider mass |
| $R_i$ | Radius of i wheel |
| $w$ | Motorcycle wheelbase |
| $x_s$ | Horizontal displacement of chassis |
| $x_3$ | Chassis local horizontal axis |
| $x_{3h}$ | Handlebar x-position in chassis frame |
| $x_{3p}$ | Footpeg x-position in chassis frame |
| $z_f$ | Fork compression |
| $z_3$ | Chassis local vertical axis |
| $z_{3h}$ | Handlebar z-position in chassis frame |
| $z_{3p}$ | Footpeg z-position in chassis frame |
| $z_s$ | Vertical displacement of chassis |
| $\alpha_r$ | Rear suspension compression angle |
| $\alpha_{r0}$ | Nominal rear suspension compression angle |
| $\epsilon$ | Caster angle |
| $\mu$ | Angular displacement of chassis |
| $\mu_1$ | Angular displacement of rear wheel |
| $\mu_4$ | Angular displacement of front wheel |

## APPENDIX A: EQUATIONS OF MOTION

The equations of motion are derived under the four assumptions described in section 2.1, namely, in plane motion, four bodies with five degrees of freedom, standing rider, and contact point under wheel centres.

We derived an equation per degree of freedom using Newton-Euler equations in the following order. First and second equations are sum of forces acting over all bodies along $x_s$ and $z_s$ respectively; third equation, is sum of torques on all bodies around centre of mass of chassis; fourth equation is sum of forces acting on front wheel along $z_f$; fifth equation is sum of torques acting on rear wheel and swing arm, around the connecting point between body 2 and 3 ($P_{23}$). Organizing the equations in matrix form, we get

$$\mathbf{M\ddot{q}} + \mathbf{m_v} = \mathbf{A_w}g + \mathbf{A_s f_s} + \mathbf{A_r f_r} + \mathbf{A_t f_t},$$

where the elements on the matrices are the following:

$$\begin{aligned}
M_{1,1} &= m_4 + m_1 + m_3 \\
M_{1,2} &= 0 \\
M_{1,3} &= ((S(\mu + \alpha_{r0} - \alpha_r) - S(\mu + \alpha_{r0}))\, l_r + C(\mu)(h - R_r) + S(\mu)\, b)\, m_1 \\
&\quad + (-z_f C(\mu + \epsilon) + C(\mu)(h - R_f) + (b - w)\, S(\mu))\, m_4 \\
M_{1,4} &= -m_4\, S(\mu + \epsilon) \\
M_{1,5} &= -l_r\, m_1\, S(\mu + \alpha_{r0} - \alpha_r) \\
M_{2,2} &= m_4 + m_1 + m_3 \\
M_{2,3} &= ((C(\mu + \alpha_{r0} - \alpha_r) - C(\mu + \alpha_{r0}))\, l_r + (-h + R_r)\, S(\mu) + C(\mu)\, b)\, m_1 \\
&\quad + (z_f S(\mu + \epsilon) + (R_f - h)\, S(\mu) + (b - w)\, C(\mu))\, m_4 \\
M_{2,4} &= -m_4\, C(\mu + \epsilon) \\
M_{2,5} &= -l_r\, m_1\, C(\mu + \alpha_{r0} - \alpha_r) \\
M_{3,3} &= \big((-2\, C(\alpha_r) + 2)\, {l_r}^2 + ((-2\, R_r + 2\, h)\, S(\alpha_{r0} - \alpha_r) + 2\, C(\alpha_{r0} - \alpha_r)\, b + \\
&\quad (-2\, h + 2\, R_r)\, S(\alpha_{r0}) - 2\, b C(\alpha_{r0}))\, l_r + {R_r}^2 - 2\, R_r\, h + b^2 + h^2\big)\, m_1 \\
&\quad + \Big((z_f)^2 + ((2\, b - 2\, w)\, S(\epsilon) + (2\, R_f - 2\, h)\, C(\epsilon))\, z_f + {R_f}^2 \\
&\quad - 2\, R_f\, h + b^2 - 2\, bw + h^2 + w^2\Big)\, m_4 + I_1 + I_2 + I_3 + I_4 \\
M_{3,4} &= ((R_f - h)\, S(\epsilon) + (w - b)\, C(\epsilon))\, m_4 \\
M_{3,5} &= \big((C(\alpha_r) - 1)\, {l_r}^2 + ((-h + R_r)\, S(\alpha_{r0} - \alpha_r) - C(\alpha_{r0} - \alpha_r)\, b)\, l_r\big)\, m_1 \\
&\quad - I_1 - I_2 \\
M_{4,4} &= m_4 \\
M_{4,5} &= 0 \\
M_{5,5} &= {l_r}^2 m_1 + I_1 + I_2
\end{aligned}$$

$$
\begin{aligned}
m_{v1,1} = & \Big(((C(\mu+\alpha_{r0}-\alpha_r)-C(\mu+\alpha_{r0}))\,l_r+(-h+R_r)\,S(\mu)+C(\mu)\,b)\,(\dot{\mu})^2 \\
& -2\,(\dot{\alpha_r})\,C(\mu+\alpha_{r0}-\alpha_r)\,(\dot{\mu})\,l_r+(\dot{\alpha_r})^2\,C(\mu+\alpha_{r0}-\alpha_r)\,l_r\Big)\,m_1 \\
& +\Big((z_f S(\mu+\epsilon)+(R_f-h)\,S(\mu)+(b-w)\,C(\mu))\,(\dot{\mu})^2-2\,C(\mu+\epsilon)\,(\dot{z_f})\,\dot{\mu}\Big)\,m_4 \\
m_{v2,1} = & \Big(((-S(\mu+\alpha_{r0}-\alpha_r)+S(\mu+\alpha_{r0}))\,l_r-S(\mu)\,b+(-h+R_r)\,C(\mu))\,(\dot{\mu})^2 \\
& +2\,(\dot{\alpha_r})\,S(\mu+\alpha_{r0}-\alpha_r)\,(\dot{\mu})\,l_r-(\dot{\alpha_r})^2\,S(\mu+\alpha_{r0}-\alpha_r)\,l_r\Big)\,m_1 \\
& +\Big((z_f C(\mu+\epsilon)+S(\mu)\,(w-b)+(R_f-h)\,C(\mu))\,(\dot{\mu})^2+2\,S(\mu+\epsilon)\,(\dot{z_f})\,\dot{\mu}\Big)\,m_4 \\
m_{v3,1} = & \Big(\big(2\,S(\alpha_r)\,{l_r}^2+(2\,S(\alpha_{r0}-\alpha_r)\,b+(-2\,h+2\,R_r)\,C(\alpha_{r0}-\alpha_r))\,l_r\big)\,(\dot{\alpha_r})\,\dot{\mu} \\
& +\big(-S(\alpha_r)\,{l_r}^2+(-S(\alpha_{r0}-\alpha_r)\,b+(h-R_r)\,C(\alpha_{r0}-\alpha_r))\,l_r\big)\,(\dot{\alpha_r})^2\Big)\,m_1 \\
& +(2\,z_f+(2\,b-2\,w)\,S(\epsilon)+(2\,R_f-2\,h)\,C(\epsilon))\,(\dot{z_f})\,(\dot{\mu})\,m_4+I_1\,\ddot{\mu}_1+I_4\,\ddot{\mu}_4 \\
m_{v4,1} = & (-z_f+(w-b)\,S(\epsilon)+(h-R_f)\,C(\epsilon))\,(\dot{\mu})^2\,m_4 \\
m_{v5,1} = & \big(-S(\alpha_r)\,{l_r}^2+(-S(\alpha_{r0}-\alpha_r)\,b+(h-R_r)\,C(\alpha_{r0}-\alpha_r))\,l_r\big)\,(\dot{\mu})^2\,m_1-I_1\,\ddot{\mu}_1
\end{aligned}
$$

$$
\begin{aligned}
A_{w1,1} = & 0 \\
A_{w2,1} = & m_4+m_1+m_3 \\
A_{w3,1} = & ((C(\mu+\alpha_{r0}-\alpha_r)-C(\mu+\alpha_{r0}))\,l_r+(-h+R_r)\,S(\mu)+C(\mu)\,b)\,m_1 \\
& +(z_f S(\mu+\epsilon)+(R_f-h)\,S(\mu)+(b-w)\,C(\mu))\,m_4 \\
A_{w4,1} = & -m_4\,C(\mu+\epsilon) \\
A_{w5,1} = & -l_r\,m_1\,C(\mu+\alpha_{r0}-\alpha_r)
\end{aligned}
$$

$$
\mathbf{A_r}=\begin{bmatrix} -1 & 0 & -1 & 0 \\ 0 & -1 & 0 & -1 \\ A_{r3,1} & A_{r3,2} & A_{r3,3} & A_{r3,4} \\ 0 & 0 & 0 & 0 \\ 0 & 0 & 0 & 0 \end{bmatrix} \qquad \mathbf{A_s}=\begin{bmatrix} 0 & 0 \\ 0 & 0 \\ 0 & 0 \\ -1 & 0 \\ 0 & -1 \end{bmatrix}
$$

$$
\begin{aligned}
A_{r3,1} = & \; S(\mu)\,x_{3p}-C(\mu)\,z_{3p} \\
A_{r3,2} = & \; C(\mu)\,x_{3p}+S(\mu)\,z_{3p} \\
A_{r3,3} = & \; S(\mu)\,x_{3h}-C(\mu)\,z_{3h} \\
A_{r3,4} = & \; C(\mu)\,x_{3h}+S(\mu)\,z_{3h}
\end{aligned}
$$

$$\mathbf{A_t} = \begin{bmatrix} -S(\mu) & -S(\mu) & -C(\mu) & -C(\mu) & C(\mu) \\ -C(\mu) & -C(\mu) & S(\mu) & S(\mu) & -S(\mu) \\ A_{t3,1} & A_{t3,2} & A_{t3,3} & A_{t3,4} & A_{t3,5} \\ C(\epsilon) & 0 & S(\epsilon) & 0 & 0 \\ 0 & A_{t5,2} & 0 & A_{t5,4} & A_{t5,5} \end{bmatrix}$$

$$\begin{aligned}
A_{t3,1} &= -z_f S(\epsilon) - b + w \\
A_{t3,2} &= C(\alpha_{r0}) l_r - l_r C(\alpha_{r0} - \alpha_r) - b \\
A_{t3,3} &= z_f C(\epsilon) - h \\
A_{t3,4} &= S(\alpha_{r0}) l_r - l_r S(\alpha_{r0} - \alpha_r) - h \\
A_{t3,5} &= -S(\alpha_{r0}) l_r + l_r S(\alpha_{r0} - \alpha_r) + h \\
A_{t5,2} &= l_r C(\alpha_{r0} - \alpha_r) \\
A_{t5,4} &= l_r S(\alpha_{r0} - \alpha_r) + R_r \\
A_{t5,5} &= -l_r S(\alpha_{r0} - \alpha_r) - R_r
\end{aligned}$$